MOTION CONTROL OF ROVER-MOUNTED MANIPULATORS

Homayoun Seraji

Jet 1 'ropulsionLaboratory

California Institute of Technology

Pasadena, CA 91109

Abstract

This paper presents a simple on-line approach for motion control of rover-mou~]trxf manipulators. An integrated kinematic model of the rover-1) lus-][[la]lil)~llatc)r system is derived which incorporates the non-holonomic rover constraint with the holonomic end-effector constraint. The redundancy introduced by the rover mobility is exploited to perform a set of user. specified additional tasks during the end-effector motion. The configuration control approach is utilized to satisfy the non-holonomic rover constraint, while accomplishing the end-effector motion and the redundancy resolution goal simultaneously. This framework allows the user to assign weighting factors to the rover movement and manipulator motion, as well as to each task specification. The computational efficiency of the contr 0 1 scheme makes it particularly suitable for real- time implementation. The proposed method is applied to a planar two jointed arm mounted on a rover, and computer simulation results are presented for illustration. [1]

1 1ntroduction

Robot manipulators mounted on mobile platforms will be utilized increasingly in both terrestrial and space applications. For instance, NASA is planning to use a tracked micro/macro manipulator arm for the Space Station Freedom, and to utilize robots mounted on micro rovers for Mars exploration. In mobile robots, the base mobility increases the size of the robot workspace substantially, and enables proper positioning of the manipulator for efficient task execution. Typical examples of mobile robots are tracked robots, gantry robots, compound robots, and wheeled *robots*.

In recent years, path planning and motion control of mobile robots have been active areas Of research [see, e.g., 1-13]. When the base mobility is provided by a track, a gantry, or another robot, the kinematics of the base platform has holonomic constraints similar to the kinematics of the manipulator itself; thus the base can effectively be treated as additional revolute or prismatic joints of the manipulator. On the other hand, wheeled mobile platforms, such as rovers, are subject to non-integrable kinematic constraints, known as *non-holonomic constraints*. Such constraints are generally caused by one or several *rolling contacts* between rigid bodies, and reflect the fact that the mobile platform must move in the direction of its main axis of symmetry. A rover is a typical non-holonomic mechanical system. It can attain any position in the plane of motion with any orientation; hence the configuration space is three-dimensional. However, the velocity of motion must always satisfy a non-holonomic constraint; thus the space of achievable velocities is two dimensional.

The problems of path planning and motion control of non-holonomic systems, such as wheeled mobile platfol-ins, have attracted considerable research in recent years [7-1 3]. In a classic paper [7], Barraquand and Latombe derive the non-holonomic rover constraint and discuss optimal maneuvering of mobile robots. Yamamoto and Yun [8 9] address coordination of locomotion and manipulation and solve the problem of following a moving surface. Wang and Kumar [10-11] associate compliance functions to the mobile manipulator joints and implement rate decomposition using screw theory. Liu and Lewis [1 2-13] develop a decentralized robust controller for trajectory tracking of the mobile manipulator end-effector.

In this paper, the configuration control methodology developed earlier [14- 15] for redundant robot control is extended to motion control of rover-mounted manipulators. The non-holonomic kinematic constraint of the rover fits naturally in the configuration control formu-

lation. The non-holonomic rover constraint, the desired end-effector motion, and the user-specified redundancy resolution goal are combined to form a set of differential kinematic constraints. These constraints are then satisfied using the configuration control approach.

The paper is structured as follows. In Section 2, we derive an *integrated* kinematic model for the rover-plus manipulator system. The motion control of the integrated system is formulated and solved using the configuration control approach in Section 3, and a simulation study is presented for illustration. Section 4 discusses the results of the paper and draws some conclusions.

2 Kinematics of Integrated Rover-plus-Manipulator System

In this section, we develop a simple kinematic model that represents the rover-plus- manipulator system. We propose a fully *integrated* kinematic representation of the rover and the manipulator, rather than treating the rover and the manipulator as two separate entities. From this view'l]oi)]t, the integrated system is composed of two closely inter acting subsystems with differ ent kinematic and dynamic characteristics. The **rover** subsystem, being a wheeled **vehicle**, is subject to non-holonomic constraints; whereas for the manipulator subsystem, the constraints **are** holonomic.

The kinematics of the rover and the manipulator sub systems are studied in the following subsections.

2.1 Non-holonomic Rover Subsystem

Consider a front-wheel-drive four-wheel rover. The rover is 1 (II)] esented by a two dimensional rect angular object translating and rotating in the plane of motion, as illustrated in Figure 1. Let $F(x_f, y_f)$ denote the midpoint between the two front wheels and $R(x_r, y_r)$ represent the midpoint between the two rear wheels of the rover, where the coordinates **are** expressed with respect **to** the fixed world frame $\{W\}$ with axes (or:, @) shown in Figure 1 The rover configuration is parameterized by the 3 x 1 vector $p = [x_f, y_f, \phi]^T$, where ϕ denotes the orientation of the main axis of the rover relative to the x-axis of the world frame.

Assuming a pure rolling contact between the rover wheels and the ground- i.e., no slipping- the velocity of point R *is* always along the main axis of the rover. Hence, we have

$$\dot{x}_r = \lambda \cos\phi \quad ; \quad \dot{y}_r = \lambda \sin\phi \qquad (1$$

where λ is a scalar, Eliminating λ, we obtain

$$\dot{x}_r \sin\phi - \dot{y}_r \cos\phi = 0 \qquad (2)$$

Equation ('2) can be expressed in terms of the coordinates (x_f, y_f) of the front point F on the rover. The coordinates of the rear point $R(x_r, y_r)$ and the front point $F(x_f, y_f)$ are related by

$$x_f = x_r + l\cos\phi \quad ; \quad y_f = y_r + l\sin\phi \qquad (3)$$

where l denotes the distance between R and F, i.e., the rover length. Thus, the velocities of R and F are related by

$$\dot{x}_f = \dot{x}_r - l\dot\phi\sin\phi \quad ; \quad \dot{y}_f = y, +l\dot\phi\cos\phi \qquad (4)$$

From equations (2) and (4), we obtain the following *non-holonomic kinematic constraint*

$$\dot{x}_f \sin\phi - \dot{y}_f \cos\phi + \dot\phi l = 0 \qquad (5)$$

or, in matrix form

$$[\sin\phi \quad -\cos\phi \quad l]\dot{p} = 0 \qquad (6)$$

where $\dot{p} = [\dot{x}_f, \dot{y}_f, \dot\phi]^T$. Equation (6) represents a natural constraint that must be satisfied by the velocity vector $\dot{p}$, [7]. Note that equation (6) is a special form of the non-holonomic constraint

$$G(p)\dot{p} = 0 \qquad (7)$$

where G is an m x n matrix and p is the n x 1 vector of generalized coordinates of the system. Note that a kinematic constraint of the form (7) is called non-holonomic if it is non-integrable; i.e., $\dot{q}$ can not be eliminated and the constraint (7) can not be rewritten in terms of q alone in the form $H(q) = O$. Otherwise, the constraint is called holonomic.

Now, the control variables of the rover are the velocity v of the front w heels and the steering angle γ between the front wheels and the main axis of the rover' Therefore, the velocity variables are related to the control variables by

$$\begin{aligned} \dot{x}_f &= v\cos(\phi + \gamma) \\ \dot{y}_f &= v\sin(\phi + \gamma) \\ \dot\phi &= \frac{v}{l}\sin\gamma \end{aligned} \qquad (8)$$

w'here the third equation is derived from the first two and the constraint (G). It is seen that at any configuration (x_f, y_f, ϕ), the space of velocities $(\dot{x}_f, \dot{y}_f, \dot\phi)$ achievable by the rover is restricted to a **two** dimensional subspace in view of the constraint (6). This implies

that the velocity vector $\dot{p}$ is completely determined by the configuration vector p and, say, $\dot{x}_f$ anti $\dot{y}_f$. Notice that the achievable configuration space (x_f, y_f, ϕ) of the rover is three-dimensional, i.e., is completely unrestricted. Finally, given $(\dot{x}_f, \dot{y}_f, \phi)$, the rover velocity v and the steering angle γ are found from equation (8) as

$$v = \left[\dot{x}_f^2 + \dot{y}_f^2\right]^{\frac{1}{2}} \quad ; \quad \gamma = \sin^{-1}\left[\frac{\dot{\phi}l}{(\dot{x}_f^2 + \dot{y}_f^2)^{\frac{1}{2}}}\right] \quad (9)$$

2,2 Holonomic Manipulator Subsystem

For simplicity of presentation, we consider a planar two link manipulator arm mounted on the rover, as illustrated in Figure 1. However, the methodology presented in this paper is general ant] is equally applicable to any type of n-jointed rover-moulted manipulator.

1 Let θ_1 and θ_2 represent the joint angles and l_1 and l_2 denote the link lengths of the manipulator arm. Consider a moving vehicle frame {V} with axes $(F\hat{x}, F\hat{y})$ attached to the rover at the front midpoint F. Let the position of the manipulator end-effector E be the primary task variable of interest. Then, the Cartesian coordinates of E with respect to the frame {V} can be expressed as

$$\hat{x}_e = l_1 \cos\theta_1 + l_2 \cos(\theta_1 + \theta_2) \quad (10)$$
$$\hat{y}_e = l_1 \sin\theta_1 + l_2 \sin(\theta_1 + \theta_2)$$

The end-effector position coordinates $X_e = [x_e, y_e]^T$ relative to the world frame {W} are given by

$$x_e = x_f + l_1 \cos(\theta_1 + \phi) + l_2 \cos(\theta_1 + \theta_2 + \phi)$$
$$y_e = y_f + l_1 \sin(\theta_1 + \phi) + l_2 \sin(\theta_1 + \theta_2 + \phi) \quad (11)$$

From equation (11), the Cartesian velocity of the end-effector in {W} is related to the rate-of-change of the configuration variables as

$$\dot{x}_e = \dot{x}_f - l_1 (\dot{\theta}_1 + \dot{\phi}) \sin(\theta_1 + \phi)$$
$$- l_2(\dot{\theta}_1 + \dot{\theta}_2 + \dot{\phi}) \sin(\theta_1 + \theta_2 + \phi)$$
$$\dot{y}_e = \dot{y}_f + l_1(\dot{\theta}_1 + \dot{\phi}) \cos(\theta_1 + \phi)$$
$$+ l_2(\dot{\theta}_1 + \dot{\theta}_2 + \dot{\phi}) \cos(\theta_1 + \theta_2 + \phi) \quad (12)$$

or, in matrix form

$$\left[\begin{array}{O} J_{m13} & J_{m14} - l_2 \sin\theta_{120} \\ J_{m23} & J_{m24} l_2 \sin\theta_{120} \end{array} \right] \left[\begin{array}{c} \dot{X}_f \\ \dot{\phi} \\ \dot{O} \end{array} \right] = \dot{X}_e \quad (13)$$

where $J_{m13} = J_{m14} = - l_1 \sin\theta_{10} - l_2 \sin\theta_{120}$, $J_{m23} = J_{m24} = l_1 \cos\theta_{10} + l_2 \cos\theta_{120}$, $\theta_{10} = \theta_1 + \phi$, $\theta_{120} =$

$\theta_1 + \theta_2 + \phi$, and $O = [\theta_1, \theta_2]^T$ is the 2 x 1 manipulator joint position vector. Equation (13) can be written in the compact form

$$J_m(q)\dot{q} = \dot{X}_e \quad (14)$$

where $J_m(q)$ is the 2 x 5 manipulator end-effector Jacobian matrix, and $q = [p^T, O^T]^T = [x_f, y_f, \phi, \theta_1, \theta_2]^T$ is the 5 x 1 configuration vector of the rover-llmullted manipulator system. Equation (14) represents a *holonomic* kinematic constraint since it can be expressed as the position constraint $H(q) = O$ in the form of equation (11).

We conclude that the kinematics of the rover-plus-manipulator system can be modeled as the non-holonomic rover constraint

$$J_r(q)\dot{q} = o \quad (15)$$

where $J_r(q) = [G(p) : 0]$, together with the holonomic manipulator constraint

$$J_m(q)\dot{q} = \dot{X}_e \quad (16)$$

Equations (15) and (16) can be combined to obtain the differential kinematic model of the integrated rover-plus-manipulator system as

$$\left[\begin{array}{c} J_r(q) \\ J_m(q) \end{array} \right] \dot{q} = \left[\begin{array}{c} 0 \\ \dot{X}_e \end{array} \right] \quad (17)$$

3 Configuration control of Integrated Rover-plus-Manipulator System

In this section, the configuration control methodology developed earlier [14-15] for redundant manipulators is extended to motion control of the rover-plus manipulator system.

Consider the integrated rover-plus-manipulator system. The integrated system is kinematically redundant with the degree-of-redundancy $n - m$, where n and m are the dimensions of $\dot{q}$ and $[0, \dot{X}_e^T]^T$ in the general case, respectively. Equation (17) can produce infinite *distinct* rover and manipulator motions $q(t)$ which yield the *same* end-effector trajectory $X_e(t)$ while satisfying the non-holonomic rover constraint. In this paper, we adopt the configuration control approach in which an appropriate motion is chosen from this infinite set which causes the integrated system to accomplish an *additional* user-specified task. This additional task is performed by direct control of a set of $r (= n - m)$ user-defined kinematic functions

$$Z = g(q) \quad (18)$$

while controlling the end-effector motion, where Z and g are $r \times 1$ vectors. The additional task constraint (18) can be expressed in the velocity form

$$J_c(q)\dot{q} = \dot{Z} \qquad (19)$$

where $J_c = \frac{\partial g}{\partial q}$ is the $r \times n$ Jacobian matrix associated with the kinematic functions Z. This approach to redundancy resolution is very general since each kinematic function $\{z_i(t)\}$ can represent a geometric variable (e.g., coordinate of a point on the system), a physical variable (such as a joint gravity torque), or an abstract mathematical function (e.g., projection of the gradient of an objective function). Furthermore, the user is not confined to a fixed set of kinematic functions and can select different $\{z_i(t)\}$ depending on the task requirements during the execution of the end-effector motion.

On combining the rover-plus-manipulator constraints (17) and the user-specified additional task constraint (19), we obtain

$$\begin{bmatrix} J_r(q) \\ J_m(q) \\ J_c(q) \end{bmatrix} \dot{q} = \begin{bmatrix} 0 \\ \dot{X}_e \\ \dot{Z} \end{bmatrix} \qquad (20)$$

or, in matrix fol-in

$$J(q)\dot{q} = \dot{X} \qquad (21)$$

where $J(q)$ is the composite $n \times n$ Jacobian matrix, and $\dot{X} = [0, \dot{X}_e^T, \dot{Z}^T]^T$ is the $n \times 1$ task velocity vector-.

Suppose that the desired end-effector velocity $\dot{X}_{de}$ and the desired rate-of-variation of the kinematic functions $\dot{Z}_d$ are specified by the user. Then we need to solve the augmented differential kinematic equation

$$J(q)\dot{q} = \dot{X}_d \qquad (z'?)$$

for q, where $\dot{X}_d = [0, \dot{X}_{de}^T, \dot{Z}_d^T]^T$. To avoid large velocities $\dot{q}$, the user can impose the velocity weighting factor $W_v = diag\{W_a, W_b\}$ on $\{\dot{p}, \dot{\theta}\}$, and attempt to minimize the weighted sum-of-squares of velocities $\| \dot{p} \|_{W_a}^2 + \| \dot{\theta} \|_{W_b}^2$. Typically, the rover movement is slower than the arm motion and W_a is larger than W_b. In addition, the user can assign priorities to the end-effector and additional task requirements and non-holonomic rover constraint by selecting the appropriate task weighting factor $W_t = diag\{W_r, W_e, W_c\}$, and seek to minimize the weighted sum of task velocity errors $\| \dot{E}_r \|_{W_r}^2 + \| \dot{E}_e \|_{W_e}^2 + \| \dot{E}_c \|_{W_c}^2$, where $\dot{E}_r = J_r \dot{q}$, $\dot{E}_e = \dot{X}_{de} - \dot{X}_e$ and $\dot{E}_c = \dot{Z}_d - \dot{Z}$ are the non-holonomic rover, end-effector, and additional task velocity errors, respectively. Hence, we seek to find the

optimal solution of equation (22) that minimizes the scalar cost function

$$L = \dot{p}^T W_a \dot{p} + \dot{\theta}^T W_b \dot{\theta} + \dot{E}_r^T W_r \dot{E}_r + \dot{E}_e^T W_e \dot{E}_e + \dot{E}_c^T W_c \dot{E}_c \qquad (23)$$

The optimal damped-least-squares solution of (22) that minimizes (23) is given by [15]

$$\dot{q} = [J^T W_t J + W_v]^{-1} J^T W_t \dot{X}_d \qquad (24)$$

Note that in the special case where $r = n - m$ and $W_v = 0$, equation (24) gives $g = J^{-1}\dot{X}_d$, assuming $det[J] \neq 0$, which is the classical inverse Jacobian solution. To correct for task-space trajectory drift which occurs inevitably due to the linearization error inherent in differential kinematic schemes, we introduce the *actual* configuration vector X in equation (24) as [15]

$$g = [J^T W_t J + W_v]^{-1} J^T W_t [\dot{X}_d + K(X_d - X)] \quad (25)$$

where K is an $(m+r) \times (m+r)$ constant diagonal matrix with zero or positive diagonal elements. Notice that for the non-holonomic rover constraint, the appropriate elements of X and X_d are set to zero since the constraint is non-integrable. The introduction of the error correction term $K(X_d - X)$ in (25) provides a "closed-loop" characteristic whereby the difference between the desired and actual configuration vectors is used as a driving term in the inverse kinematic transformation. Note that for task-space trajectories with constant final values, $\dot{X}_d(t) = 0$ for $t \geq \tau$ where τ is the motion duration, using (24) we obtain $\dot{q}(t) = 0$ for $t \geq \tau$; i.e., the manipulator and rover degrees of-freedom will cease motion for $t \geq \tau$ and any task tracking-error at $t = \tau$ will continue to exist for $t > \tau$. However, by using (25) the manipulator and rover degrees-of-freedom continue to move for $t \geq \tau$ until the desired configuration vector is reached, i.e., $X \rightarrow X_d$ as $t \rightarrow \infty$, [15]. The value of K determines the rate of convergence of X to X_d.

The proposed damped-least-squares configuration control scheme provides a general and unified framework for motion control of the integrated rover-plus-manipulator system. This scheme allows independent weighting of rover movement and manipulator motion, and enables a wide range of redundancy resolution goals to be accomplished. Note that multiple goals can be defined for redundancy resolution and weighted appropriately based on the current task requirements.

Let us now re-visit the two-jointed manipulator arm mounted on the rover as illustrated in Figure 1. This integrated system has the degree-of-redundancy $r = n - m = 2$, and therefore two configuration-dependent kinematic functions $z_1(q)$ and $z_2(q)$ can be specified and controlled independently of the end-effector motion and the non-holonomic rover constraint. For this system,

we choose the rover orientation ϕ relative to the world frame and the manipulator elbow angle ψ between the upper-arm and forearm as tile additional task variables. Hence

$$z_1(q) = \phi \quad ; \quad z_2(q) = \psi = 180 - \theta_2 \qquad (26)$$

or, in velocity form

$$\begin{bmatrix} 0 & 0 & 1 & 0 & 0 \\ 0 & 0 & 0 & 0 & -1 \end{bmatrix} \dot{q} = \begin{bmatrix} \dot{\phi}_d \\ \dot{\psi}_d \end{bmatrix} \qquad (27)$$

where $\dot{q} = [\dot{x}_f, \dot{y}_f, \dot{\phi}, \dot{\theta}_1, \dot{\theta}_2]^T$, and $\dot{\phi}_d$ and $\dot{\psi}_d$ are the desired rate-of-variation of ϕ and ψ, respectively. On combining the rover-plus-manipulator model (17) with the additional task specifications (27), we obtain

$$\begin{vmatrix} \sin\phi & -\cos\phi & 1 & 0 & 0 \\ 1 & 0 & J_{23} & J_{24} & J_{25} \\ o & 1 & J_{33} & J_{34} & J_{35} \\ o & 0 & 1 & 0 & 0 \\ 0 & 0 & 0 & 0 & -1 \end{vmatrix} \begin{vmatrix} \dot{x}_f \\ \dot{y}_f \\ \dot{\phi} \\ \dot{\theta}_1 \\ \dot{\theta}_2 \end{vmatrix} \begin{vmatrix} 0 \\ \dot{x}_{de} \\ \dot{y}_{de} \\ \dot{\phi}_d \\ \dot{\psi}_d \end{vmatrix} \qquad (28)$$

where $J_{23} = J_{24} = -l_1 \sin\theta_{10} - l_2 \sin\theta_{120}$; $J_{33} = J_{34} = l_1 \cos\theta_{10} + l_2 \cos\theta_{120}$; $J_{25} = -l_2 \sin\theta_{120}$; $J_{35} = l_2 \cos\theta_{120}$; $\theta_{10} = \theta_1 + \phi$; $\theta_{120} = \theta_1 + \theta_2 + \phi$. Equation (28) represents a set of five equations in the five unknown elements of $\dot{q}$ that can l~csol J'cel LlsillC t}lcc181111)ccl- least-squares configuration control approach described earlier in this section. By direction calculation, the determinant of the 5 x 5 augmented Jacobian matrix appearing on the left-hand side of (28) is found to be

$$\det[J] = l_1 \cos\theta_1 + l_2 \cos(\theta_1 + \theta_2) = \hat{x}_e \qquad (29)$$

Therefore, J is non-singular and (28) can be solved exactly provided that $\hat{x}_e \neq 0$; i.e., the end-effector E dots not lie on the $F\hat{y}$ axis of the vehicle frame $\{V\}$.

Now, suppose that the rover length is $l = 20$cm and the link lengths are $l_1 = l_2 = 10$cm. Let the initial configuration of the rover-plus-manipulator system be given by

$$q^i = \{x_f = 30cm, y_f = 15cm, \phi = 0°, \theta_1 = -75°, \theta_2 = 150°\}$$

This yields the initial task vector

$$X^i = \{x_e = 35.18cm, y_e = 15cm, \phi = 0°, \psi = 30°\}$$

as shown in Figure 2. Suppose that the desired final task vector at time $\tau = 1$ second is specified as (see Figure 2)

$$X^f = \{x_e = 65.18cm, y_e = 45cm, \phi = 30°, \psi = 90°\}$$

This corresponds to a rapid end-effector motion of $\{(\Delta x_e)^2 + (\Delta y_e)^2\}^{\frac{1}{2}} = 42.4$cm in one second. Notice

that the target end-effector position is *not* attainable without rover motion. Task-space motion trajectories are specified as

$$x_d(t) = \begin{cases} x^i + \frac{x^f - x^i}{\tau} \cdot t & , \quad \text{for } t \leq \tau \\ x^f & , \quad \text{for } t > \tau \end{cases} \qquad (30)$$

where (x^i, x^f) are the initial and final values and τ is the duration of motion. Similar trajectories are specified for $y_d(t)$, $\phi_d(t)$, and $\psi_d(t)$. These trajectories produce a straight-line end-effector motion in Cartesian space from (x_e^i, y_e^i) to (x_e^f, y_e^f). Notice that the target elbow angle $\psi = 90°$ gives maximum end-effector manipulability at the final configuration.

A computer simulation study is performed to calculate the required configuration variables $q(t) = \{x_f(t), y_f(t), \phi(t), \theta_1(t), \theta_2(t)\}$ to accomplish the tasks of end-effector motion, and ϕ and ψ control, while satisfying the non-holonomic rover constraint. In the simulation, we set, $\tau = 1, \Delta t = 0.01$, $W = diag\{1, 1, 1, 1, 1\}$, $W_v = diag\{0, 0, 0, 0, 0\}$, and $K = diag\{0, 0.1, 0.1, 0, 0\}$. The simulation results are shown in Figures 3a-3d. The path traversed by the end-effector E is shown in Figure 3a. It is seen that the end-effector moves on a straight line from (x_e^i, y_e^i) to (x_e^f, y_e^f), as specified. Figure 3b verifies that the rover orientation ϕ and the elbow angle ψ change from their initial values to the specified final values in one second, as desired. The path traversed by the rover front mid-point F and the variations of the arm joint angles θ_1 and θ_2 are depicted in Figures 3c and 3d. The rover non-holonomic constraint function $f = \dot{x}_f \sin\phi - \dot{y}_f \sin\phi - \dot{\phi}l$ is computed and is found to be equal to zero throughout the motion; i.e., the rover constraint is satisfied. Note that the required rover velocity v and steering angle γ can be computed from equation (9).

4 Conclusions

Effective utilization of rover-IIIoullted manipulators requires that the motion of the rover and the manipulator be planned and controlled in a coordinated manner. This coordination poses a technically challenging problem since the rover and the manipulator possess very different kinematic characteristics. Because the rover is a wheeled vehicle, it is subject to non-holonomic constraints, that is, constraints expressible in terms of generalized velocities and not generalized coordinates. This is in contrast to the manipulator, which possesses a holonomic structure with constraints depending directly on generalized coordinates This kinematic dissimilarity substantially increases the difficulty of coordinated motion planning and control problem for rover-mounted manipulators.

In this paper, a simple scheme is presented for *on-line* control of rover--uoullted manipulators. The configuration control approach is extended to incorporate the non-holonomic rover constraint with the desired end-effector motion and the user-specifkxi redundancy resolution goal. The key advantages of the present approach over the previous schemes are its flexibility, simplicity, and computational efficiency. The ability to change the task specifications and the task weighting factors 07 L-*line* based on the user requirements provides a flexible framework for mobile robot control. Furthermore, in contrast to previous approaches which arc suitable for off-line motion planning, the simplicity of the present approach leads to computational efficiency which is essential for on-line control in real-ti~rlc implementations.

References

[1] W. 1'. Carriker, 1). K. Khosla, and B. 11. Krogh: "Path planning for mobile manipulators for multiple task execution," IEEE Trans. ou Robotics aud Automation, Vol. 7, No.3, pp. 403-408, June 1991.

[2] W. F. Carriker, 1'. K. Khosla, aud B. II. Krogh: "The use of simulated annealing to solve the mobile manipulator path planning problem," Proc. IEEE Intern. Conf. on Robotics and Automation, pp. 204-209, May 1990.

[3] F. G. Pin and J. C. Culioli: "Optimal positioning of redundant manipulator - platform systems for maximum task efficiency," Proc. Intern. Symposium on Robotics and Manufacturing, pp. 489-495, July 1990.

[4] F. G. Pin and J. C. Culioli: "Multi-criteria position and configuration optimization for redundant platform/manipulator systems," Proc. IEEE Workshop on Intelligent Robots and Systems, pp. 103 107, July 1990.

[5] N. A. M. Hootsmans and S. Dubowsky: "Large motion control of mobile manipulators including vehicle suspension characteristics," Proc. IEEE Intern. Conf. on Robotics and Automation, pp. 233G-?341, April 1991.

[6] 11. Scraji: "An on-line approach to coordinated mobility and manipulation," Proc. IEEE Intern. Conf. on Robotics and Automation, Vol. 1, pp. 28 35, Atlanta, May 1993.

[7] J, Barraquand and J. C. Latombe: "On nonholonomic mobile robots and optimal maneuvering, "

Proc. 4th IEEE Intern. Symposium on Intelligent Control, pp. 340-347, Albany, September 1989.

[8] Y. Yamamoto and X. Yun: "Coordinating locomotiou and manipulation of a mobile manipulator," Proc. 31st IEEE Conf. on Decision and Control, pp. 2643-2648, Tucson, December 1992.

[9] Y. Yamamoto and X. Yun: "Control of mobile manipulators following a moving surface," Proc. IEEE Intern. Conf. on Robotics and Automation, Vol. 3, pp. 1-6, Atlanta, May 1993.

[10] C. C. Wang, N. Sarkar, and V. Kumar: "Rate kinematics of mobile manipulators," Proc. 22nd Biennial ASME Mechanisms Conf., pp. 225 232, Scottsdale, September 1992.

[11] C. C. Wang and V. Kumar: "Velocity control of mobile manipulators," Proc. IEEE Intern. Conf. on Robotics and Automation, Vol. 2, pp. 7] 3-718, Atlanta, May 1993.

[12] K. Liu and F. J, Lewis: "Control of mobile robot with onboard manipulator," Proc. Intern. Symposium on Robotics and Manufacturing, Vol. 4, pp. 539546, Santa Fe, November 1992.

[13] S. Jagannathan, F. L. Lewis, and 1<. Liu: "Modeling, control and obstacle avoidance of a mobile robot with an onboard manipulator, " Proc. IEEE Intern. Symp. on Intelligent Control, Chicago, August 1993.

[14] II. Scraji: "Configuration control of redundant manipulators: Theory and implementation," IEEE Trans. on Robotics and Automation, Vol. 5, No. 4, pp. 472490, 1989.

[15] II. Scraji and R. Colbaugh: "Impr oved configuration control for redundant robots, " Journal of Robotic Systems, Vol. 7, No. 6, pp. 897-9?8, 1990.
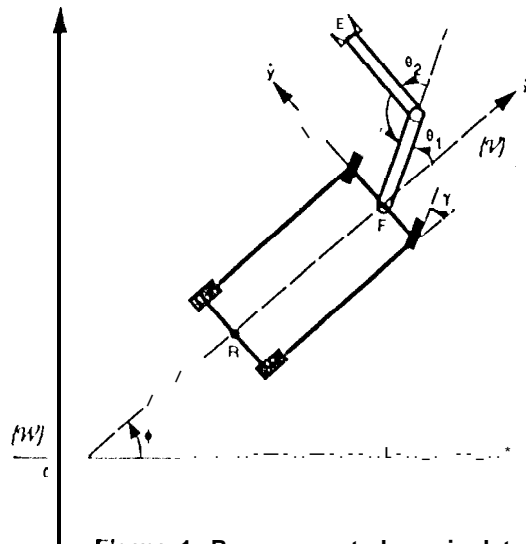
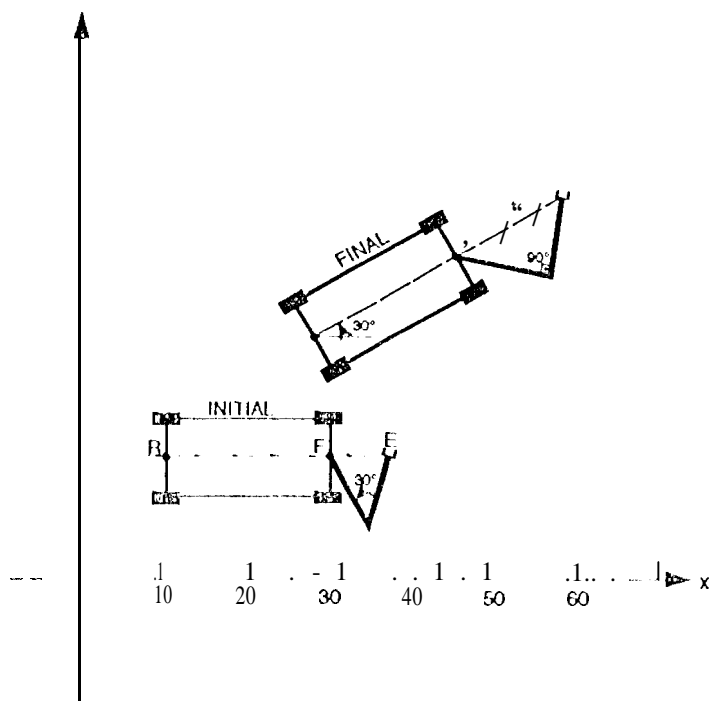Figure 1. Rover-mounted manipulator

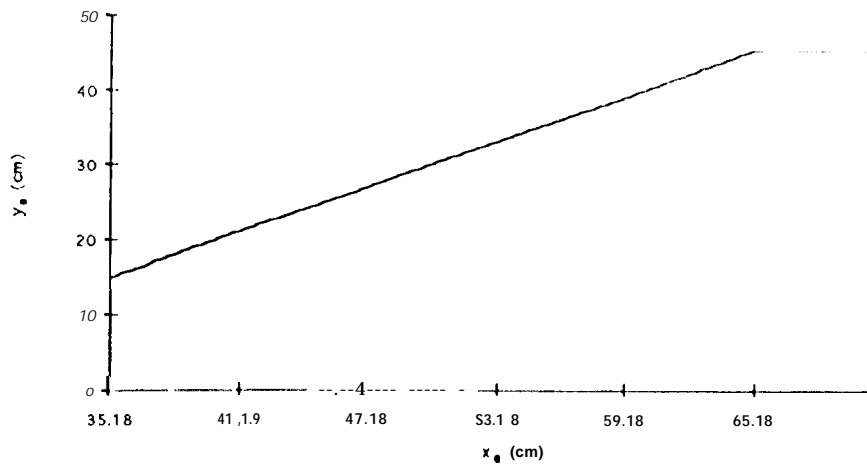Figure 2. Initial and final configurations in the emulation study

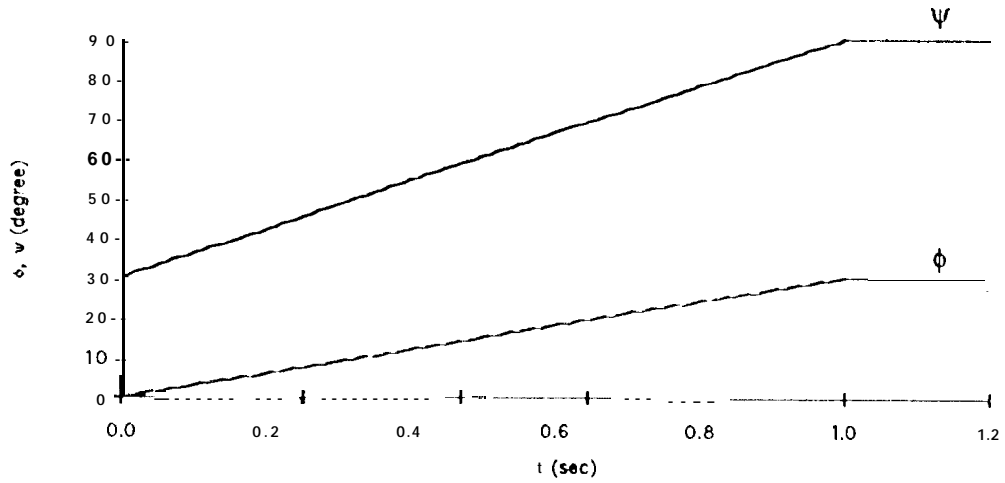Figure 3a. Motion trajectory of the end-off ector E

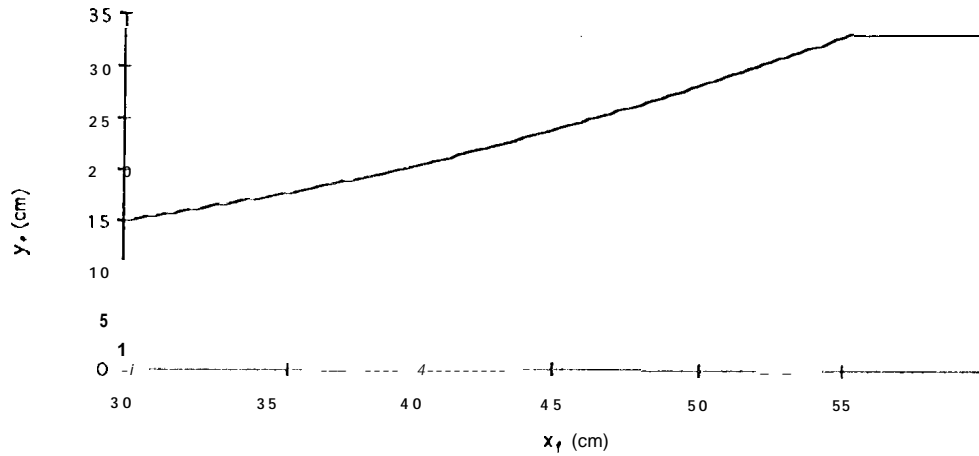**Figure 3b. Variations of the rover orientation φ and elbow angle ψ**

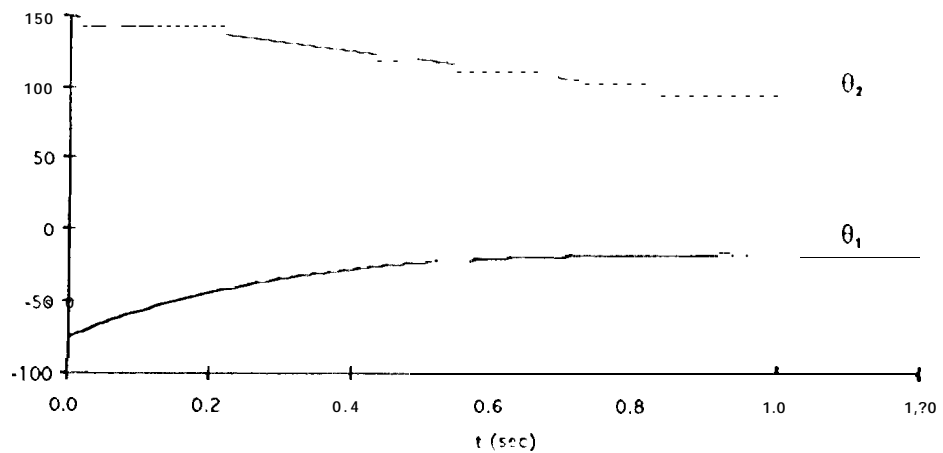**Figure 3c. Motion trajectory of the rover front midpoint F**

Figure 3d. Variations of the arm joint angles θ₁ and θ₂